Hydrogen induced optically-active defects in silicon photonic nanocavities

S. Boninelli,[1,*] G. Franzò,[1] P. Cardile,[1] F. Priolo,[1,2,3] R. Lo Savio,[4] M. Galli,[4] A. Shakoor,[5,7] L. O'Faolain,[5] T. F. Krauss,[5,8] L. Vines,[6] and B. G. Svensson[6]

[1]*MATIS IMM CNR via S. Sofia 64, 95123 Catania, Italy*
[2]*Dipartimento di Fisica e Astronomia, Università di Catania, via S. Sofia 64, 95123 Catania, Italy*
[3]*Scuola Superiore di Catania, Via Valdisavoia 9, 95123 Catania, Italy*
[4]*Dipartimento di Fisica, Università di Pavia, via Bassi 6, 27100 Pavia, Italy*
[5]*SUPA, School of Physics and Astronomy, University of St. Andrews, Fife KY16 9SS, St. Andrews, UK*
[6]*Department of Physics, University of Oslo, Kristen Nygaards hus, Gaustadallèen 23a, 0373 OSLO, Norway*
[7]*Now at: NTT Basic Research Laboratories, NTT Corporation, 3-1 Morinosato Wakamiya, Atsugi, Kanagawa 243-0198, Japan*
[8]*Now at Department of Physics, University of York, York, YO10 5DD, UK*
[*]*simona.boninelli@ct.infn.it*

Abstract: We demonstrate intense room temperature photoluminescence (PL) from optically active hydrogen- related defects incorporated into crystalline silicon. Hydrogen was incorporated into the device layer of a silicon on insulator (SOI) wafer by two methods: hydrogen plasma treatment and ion implantation. The room temperature PL spectra show two broad PL bands centered at 1300 and 1500 nm wavelengths: the first one relates to implanted defects while the other band mainly relates to the plasma treatment. Structural characterization reveals the presence of nanometric platelets and bubbles and we attribute different features of the emission spectrum to the presence of these different kind of defects. The emission is further enhanced by introducing defects into photonic crystal (PhC) nanocavities. Transmission electron microscopy analyses revealed that the isotropicity of plasma treatment causes the formation of a higher defects density around the whole cavity compared to the ion implantation technique, while ion implantation creates a lower density of defects embedded in the Si layer, resulting in a higher PL enhancement. These results further increase the understanding of the nature of optically active hydrogen defects and their relation with the observed photoluminescence, which will ultimately lead to the development of intense and tunable crystalline silicon light sources at room temperature.

OCIS codes: (160.5298) Photonic crystals; (160.6000) Semiconductor materials; (250.5230) Photoluminescence; (160.2220) Defect-center materials.

References and links

1. F. Iacona, D. Pacifici, A. Irrera, M. Miritello, G. Franzò, F. Priolo, D. Sanfilippo, G. Di Stefano, and P. G. Fallica, "Electroluminescence at 1.54 μm in Er-doped Si nanocluster-based devices," Appl. Phys. Lett. **81**(17), 3242–3244 (2002).
2. Y. Gong, M. Makarova, S. Yerci, R. Li, M. J. Stevens, B. Baek, S. W. Nam, L. Dal Negro, and J. Vuckovic, "Observation of transparency of erbium-doped silicon nitride in photonic crystal nanobeam cavities," Opt. Express **18**(13), 13863–13873 (2010).
3. G. Franzò, A. Irrera, E. Ceretta Moreira, M. Miritello, F. Iacona, D. Sanfilippo, G. Di Stefano, P. G. Fallica, and F. Priolo, "Electroluminescence of silicon nanocrystals in MOS structures," Appl. Phys., A Mater. Sci. Process. **74**(1), 1–5 (2002).
4. A. Marconi, A. Anopchenko, M. Wang, G. Pucker, P. Bellutti, and L. Pavesi, "High power efficiency in Si-nc/SiO_2 multilayer light emitting devices by bipolar direct tunneling," Appl. Phys. Lett. **94**, 221110 (2009).
5. L. Pavesi, L. Dal Negro, C. Mazzoleni, G. Franzò, and F. Priolo, "Optical gain in silicon nanocrystals," Nature **408**(6811), 440–444 (2000).
6. W. L. Ng, M. A. Lourenço, R. M. Gwilliam, S. Ledain, G. Shao, and K. P. Homewood, "An efficient room-temperature Si-based light-emitting diode," Nature **410**, 192–194 (2001).

#201767 - $15.00 USD Received 22 Nov 2013; revised 10 Feb 2014; accepted 21 Feb 2014; published 7 Apr 2014

7. H. Rong, R. Jones, A. Liu, O. Cohen, D. Hak, A. Fang, and M. Paniccia, "A continuous-wave Raman silicon laser," Nature **433**(7027), 725–728 (2005).
8. S. G. Cloutier, P. A. Kossyrev, and J. Xu, "Optical gain and stimulated emission in periodic nanopatterned crystalline silicon," Nat. Mater. **4**(12), 887–891 (2005).
9. J. Liu, X. Sun, R. Camacho-Aguilera, L. C. Kimerling, and J. Michel, "Ge-on-Si laser operating at room temperature," Opt. Lett. **35**(5), 679–681 (2010).
10. R. E. Camacho-Aguilera, Y. Cai, N. Patel, J. T. Bessette, M. Romagnoli, L. C. Kimerling, and J. Michel, "An electrically pumped germanium laser," Opt. Express **20**(10), 11316–11320 (2012).
11. F. Priolo, T. Gregorkiewicz, M. Galli, and T. F. Krauss, "Silicon nanostructures for photonics and photovoltaics," Nat. Nanotechnol. **9**(1), 19–32 (2014).
12. A. Shakoor, R. Lo Savio, P. Cardile, S. L. Portalupi, D. Gerace, K. Welna, S. Boninelli, G. Franzò, F. Priolo, T. F. Krauss, M. Galli, and L. O'Faolain, "Room temperature all-silicon photonic crystal nanocavity light emitting diode at sub-bandgap wavelengths," Laser Photonics Rev. **7**(1), 114–121 (2013).
13. H. Weman, B. Monemar, G. S. Oehrlein, and S. J. Jeng, "Strain-induced quantum confinement of carriers due to extended defects in silicon," Phys. Rev. B Condens. Matter **42**(5), 3109–3112 (1990).
14. J. Weber, "Defect generation during plasma treatment of semiconductors," Physica B **170**(1-4), 201–217 (1991).
15. A. V. Mudryi, F. P. Korshunov, A. I. Patuk, I. A. Shakin, T. P. Larionova, A. G. Ulyashin, R. Job, W. R. Fahrner, V. V. Emtsev, V. Yu. Davydov, and G. Oganesyan, "Low-temperature photoluminescence characterization of defects formation in hydrogen and helium implanted silicon at post-implantation annealing," Physica B **308–310**, 181–184 (2001).
16. J. Weber, T. Fischer, E. Hieckmann, M. Hiller, and E. V. Lavrov, "Properties of hydrogen induced voids," J. Phys. Condens. Matter **17**(22), S2303–S2314 (2005).
17. J. Grisolia, G. Ben Assayag, A. Claverie, B. Aspar, C. Lagahe, and L. Laanab, "A transmission electron microscopy quantitative study of the growth kinetics of H platelets in Si," Appl. Phys. Lett. **76**(7), 852–854 (2000).
18. X. Hebras, P. Nguyen, K. K. Bourdelle, F. Letertre, N. Cherkashin, and A. Claverie, "Comparison of platelets formation in hydrogen and helium-implanted silicon," Nucl. Instrum. Methods B **262**(1), 24–28 (2007).
19. C. Ghica, L. C. Nistor, M. Stefan, D. Ghica, B. Mironov, S. Vizireanu, A. Moldovan, and M. Dinescu, "Specificity of defects induced in siliconby RF-plasma hydrogenation," Appl. Phys., A Mater. Sci. Process. **98**(4), 777–785 (2010).
20. C. Ghica, L. C. Nistor, S. Vizireanu, and G. Dinescu, "Annealing of hydrogen-induced defects in RF-plasma-treated Si wafers: ex situ transmission electron microscopy studies," J. Phys. D Appl. Phys. **44**, 295401 (2011).
21. N. M. Johnson, F. A. Ponce, R. A. Street, and R. J. Nemaich, "Defects in single-crystal silicon induced by hydrogenation," Phys. Rev. B Condens. Matter **35**(8), 4166–4169 (1987).
22. H. Weman, J. L. Lindström, G. S. Oerhlein, and B. G. Svensson, "Reactive ion and plasma etching induced extended defects in silicon studied with photoluminescence," J. Appl. Phys. **67**(2), 1013–1021 (1990).
23. R. Lo Savio, S. L. Portalupi, D. Gerace, A. Shakoor, T. F. Krauss, L. O'Faolin, L. C. Andreani, and M. Galli, "Room-temperature emission at telecom wavelengths from silicon photonic crystal nanocavities," Appl. Phys. Lett. **98**, 201106 (2011).
24. A. Shakoor, R. Lo Savio, S. L. Portalupi, D. Gerace, L. C. Andreani, M. Galli, T. F. Krauss, and L. O'Faolain, "Enhancement of room temperature sub-bandgap light emission from silicon photic crystal nanocavity by Purcell effect," Physica B **407**(20), 4027–4031 (2012).
25. Y. Akahane, T. Asano, B.-S. Song, and S. Noda, "High-Q photonic nanocavity in a two-dimensional photonic crystal," Nature **425**(6961), 944–947 (2003).
26. N.-V.-Q. Tran, S. Combrié, and A. De Rossi, "Directive emission from high-Q photonic crystal cavities through band folding," Phys. Rev. B **79**, 041101 (2009).
27. S. L. Portalupi, M. Galli, C. Reardon, T. F. Krauss, L. O'Faolain, L. C. Andreani, and D. Gerace, "Planar photonic crystal cavities with far-field optimization for high coupling efficiency and quality factor," Opt. Express **18**(15), 16064–16073 (2010).
28. S. Boninelli, A. Claverie, G. Impellizzeri, S. Mirabella, F. Priolo, E. Napolitani, and F. Cristiano, "Evidences of F-induced nanobubbles as sink for self-interstitials in Si," Appl. Phys. Lett. **89**, 171916 (2006).
29. S. Boninelli, G. Impellizzeri, S. Mirabella, F. Priolo, E. Napolitani, N. Cherkashin, and F. Cristiano, "Formation and evolution of F nanobubbles in amorphous and crystalline Si," Appl. Phys. Lett. **93**, 061906 (2008).
30. T. Höchbauer, A. Misra, M. Nastasi, and J. W. Mayer, "Physical mechanisms behind the ion-cut in hydrogen implanted silicon," J. Appl. Phys. **92**(5), 2335–2342 (2002).
31. N. Hauke, T. Zabel, K. Müller, M. Kaniber, A. Laucht, D. Bougeard, G. Abstreiter, J. J. Finley, and Y. Arakawa, "Enhanced photoluminescence emission from two-dimensional silicon photonic crystal nanocavities," New J. Phys. **12**, 053005 (2010).
32. A. Shakoor, "Silicon nanocavity light emitters at 1.3-1.5 μm wavelength," PhD thesis, University of St. Andrews (2013).

1. Introduction

The aim of achieving higher data processing speeds and bandwidths is the driving force for the research and development of integrated photonic devices that use photons as data carriers. A single material platform is ultimately desired for the realization of such on-chip photonic components in order to provide a high integration density and to simplify fabrication

#201767 - $15.00 USD Received 22 Nov 2013; revised 10 Feb 2014; accepted 21 Feb 2014; published 7 Apr 2014

complexity. Silicon is the natural material choice for this purpose due to its maturity and compatibility with microelectronic circuitry. Unfortunately, Si has poor light emission efficiency due to its indirect bandgap, which hampers the use of Si as a single material platform for photonic functionalities. A number of promising approaches have been taken in the past to enhance the Si emission [1–11]. Unfortunately, none of these combine all the features required from a practical on-chip light source, namely: room temperature operation, electrical injection, sub-bandgap emission, small size, high output power, spectral purity and tunability. Recently, we have demonstrated a Si nano light emitting diode (LED) that has all of the features listed above [12], except for the high output power. This device is based on the introduction of optically active hydrogen defects in crystalline silicon and Purcell enhancement via a PhC cavity. To further enhance the emission and to bring it up to practical levels, it is necessary to better understand the nature of these defects and the role they play in the emission process, which is a topic of considerable debate [13–22].

In the present paper we provide a better understanding of the emission process and its origin by combining different analytical techniques (transmission electron microscopy, secondary ion mass spectrometry and photoluminescence). Moreover a detailed analysis of the kinds of defects and their contribution in creating the luminescence bands is presented.

2. Experimental

We used Silicon on insulator (SOI) samples from SOITEC, consisting of a 220 nm thick Si film on a 2 μm thick SiO_2 layer. The plasma treatments were performed by using a reactive ion etching system. The plasma power was fixed at 40 W and the treatment duration at 30 min. The chamber pressure was kept at 0.1 mbar and all treatments were carried out at room temperature. Two different gases were used, i.e. pure hydrogen and pure argon.

Hydrogen implantation was done by using a 400 kV HVEE Ion Implanter at an energy of 8 keV (which locates the implantation peak and corresponding defect band in the center of the Si layer) and with doses in the range $1x10^{14}$ – $5x10^{15}$ H/cm^2. The highest dose yields a hydrogen peak concentration of about $4.3x10^{20}$ H/cm^3. Moreover, some of the samples were implanted with multiple H implants (in the energy range 5 - 15 keV, and with doses in the range $2.3x10^{15}$ – $3.5x10^{15}$/cm^2) in order to produce an almost constant H profile across the entire Si layer and to increase the optically active defects density. In order to understand the thermal evolution of the structural defects and to correlate this evolution to their light emitting properties, both plasma treated and implanted SOI samples were annealed at different temperatures (in the range 300 – 500 °C) for 30 min in a conventional furnace under a controlled forming gas (FG) atmosphere.

To observe the damage induced by H plasma or H implantation on SOI, we performed cross sectional (CS) transmission electron microscopy (TEM) measurements with a JEOL JEM 2010 instrument operating at an acceleration voltage of 200 kV. All CS TEM samples were prepared using standard mechanical grinding and ion milling.

The H atomic concentration was determined by secondary ion mass spectrometry (SIMS), employing a Cameca IMS7f microanalyzer. A beam of 15 keV Cs^+ ions was rastered over a surface area of 130 × 130 μm^2 and secondary ions were collected from the central part of the sputtered crater. Crater depths were measured with a Dektak 8 stylus profilometer, and a constant erosion rate was assumed when converting sputtering time to sample depth. Calibration of the H signal was performed using an implanted reference sample.

Luminescence measurements were performed in a confocal μPL setup where a 640 nm CW laser was focussed onto the sample with a high numerical aperture objective (NA = 0.8). The emitted light from the sample was collected by the same objective and filtered by a pin-hole. The filtered light was then fed into a grating spectrometer with an InGaAs detector. Further details on the characterization methods can be found elsewhere [23, 24].

L3 PhC cavities, that are known to have very high Q/V values, were fabricated on Silicon on Insulator (SOI) material using electron beam lithography and reactive ion etching with a CHF_3/SF_6 gas mixture. The buried oxide layer underneath the photonic-crystal slab was selectively removed using diluted hydrofluoric acid to leave the photonic crystal section as a

#201767 - $15.00 USD Received 22 Nov 2013; revised 10 Feb 2014; accepted 21 Feb 2014; published 7 Apr 2014

suspended silicon membrane. Several PhC nanocavities were fabricated with a lattice constant a varying between 340 and 420 nm and a normalized hole radius (r/a) of 0,285. The two holes adjacent to the cavity were reduced in size and displaced laterally to increase the quality factor of the cavity [25]. To obtain the maximum out-coupling efficiency in the vertical direction, we applied a far-field optimization technique, whereby alternating holes around the cavity are enlarged to form a second order grating. This folds back the k-vector components near the edge of the Brillouin zone, outside the light emission cone, into the centre, resulting in an increase of the vertical emission efficiency [26, 27]. We used an enlargement of 15 nm in hole radius to provide maximal vertical out-coupling efficiency.

3. Results and discussion

It is known that H plasma treated samples [13,14] and H implanted samples [15,16] show a low-temperature broad band luminescence characterized by two main peaks centred at about 1300 and 1450 nm. The damage associated with the incorporation of hydrogen in crystalline Si mainly consists of {100} and {111} platelets and nano-bubbles [17–20].

The relationship between the broad PL band observed in hydrogen-enriched samples and hydrogen-induced damage is controversial and it is not clear whether to ascribe the PL emission to the damage induced by the plasma treatment, to the creation of platelets, to the strain field associated with the defects or simply to the passivation provided by hydrogen [13, 16, 21, 22].

Here we aim to better understand these issues with the goal of utilizing this approach to develop an efficient light source based on crystalline silicon.

3.1 Plasma treated SOI

In order to study the correlation between the role of the plasma species and the PL emission, we treated two different SOI samples with an Ar and H_2 plasma. In Fig. 1 the CS TEM images of the two samples are shown. The images were acquired in off-Bragg defocused bright field conditions in order to avoid the background strain contrast around each defect and to highlight the Fresnel contrast between the edge of the void itself and the surrounding crystalline Si matrix [17, 28, 29]. The TEM of Ar plasma treated SOI [Fig. 1(a)] reveals the presence of a damaged layer extending up to 30 nm below the surface where the defect population consists of platelets that are oriented along the {111} and (001) planes, with a mean diameter of ~10 nm. A different scenario is shown in the image of the H_2 plasma treated sample [Fig. 1(b)]. Indeed, the damaged region, extending up to ~40 nm below the surface, presents different defects: in the first 10 nm the damage consists of bubbles with a mean diameter of a few nm, while further down, a buried band of platelets is found. The thickness of the band is 30 nm, the mean diameter of platelets lying on (001) is 15 nm while the mean diameter of platelets lying on {111} is 10 nm. Energy filtered TEM (not shown) reveals that the 7 nm thick amorphous layer found on the top Si surface of the H plasma treated sample consists of a SiO_x film. Since we observed the presence of this layer only on the surface of all the H treated samples and not on the Ar treated ones, we believe that it may be due to the hydrogenation treatment, as already speculated by Ghica et al. [20].

#201767 - $15.00 USD Received 22 Nov 2013; revised 10 Feb 2014; accepted 21 Feb 2014; published 7 Apr 2014

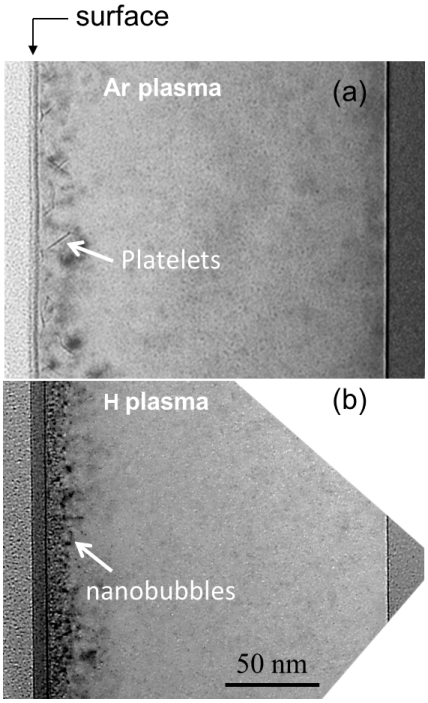

Fig. 1. Cross sectional TEM of SOI after the exposure to a 40 W plasma treatment for 30 min in Ar (a) and H_2 (b).

In order to correlate the structural and the optical properties, we carried out room temperature PL measurements of the samples.

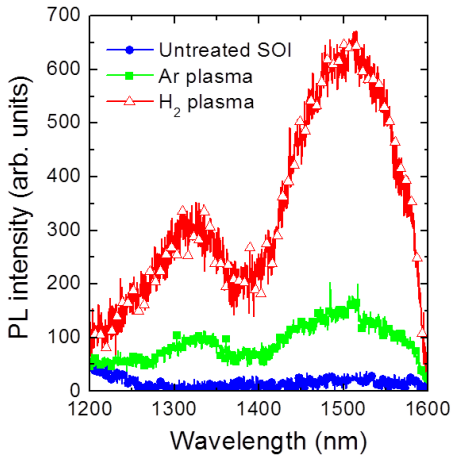

Fig. 2. Photoluminescence spectra of H-plasma (red triangles) and Ar-plasma treated (green squares) samples compared to that of an untreated SOI taken as a reference (blue circles).

In Fig. 2, the PL spectra of H-treated (red triangles), Ar-treated (green squares), and untreated SOI (blue circles) are shown. The PL spectra of the plasma treated samples show a broad band with two main peaks at ~1300 nm and at ~1500 nm, with the PL emission from H treated sample being more intense than the Ar-treated ones.

Moreover, the PL due to defects created by the H-plasma treatment was found to be stable, with only a moderate decrease in the emission observed over 6 months, while the PL from the Ar-treated samples completely disappears on the same timescale. The comparison

#201767 - $15.00 USD Received 22 Nov 2013; revised 10 Feb 2014; accepted 21 Feb 2014; published 7 Apr 2014

reveals that the creation of defects alone is sufficient to obtain light emission in SOI substrates. However, their passivation by hydrogen enhances and stabilizes the light emission, since hydrogen removes non-radiative recombination centers. For this reason, we focus our attention only on the H-plasma treatment.

Since hydrogen has a key role in the defects passivation, we studied the thermal evolution of hydrogen treated samples by performing annealing in forming gas atmosphere in the temperature range 350 - 500 °C for 30 min. In Fig. 3(a), the TEM micrograph of a sample annealed at 350 °C is reported; the damaged layer is slightly reduced to ~30 nm while the band of nanobubbles stays constant at ~10 nm. This reduction of the damaged layer is due to the shrinking of the platelets band by ~10 nm. Indeed, the mean diameter of {111} platelets is reduced to 6 nm while the (001) platelets are completely dissolved. Finally, after a thermal treatment at 500 °C for 30 min, we observe a strong reduction of the damage depth and a dissolution of the platelets. This is in good agreement with previous reports [20].

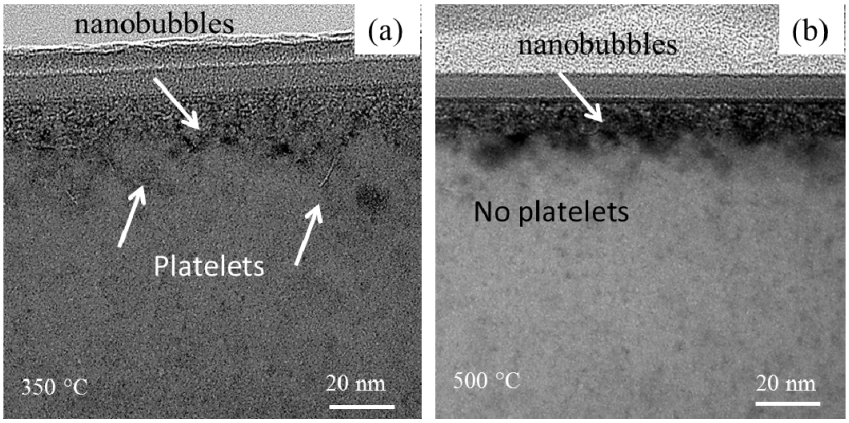

Fig. 3. Cross sectional TEM of the H-plasma treated SOI after annealing at 350 °C (a) and 500 °C (b) for 30 min in forming gas.

In Fig. 4, we show the corresponding depth profiles of hydrogen in the plasma treated samples measured by SIMS for not-annealed (black squares), 350 °C (red circles) and 500 °C (blue triangles) annealed samples. We note a high H accumulation near the surface with a long tail extending to a depth of 150 nm. The H peak close to the surface, seen at a depth of 7 nm (peak concentration of ~9.7×10^{21} H/cm^3), is due to H agglomeration at the interface between the native SiO_2 and the Si layers. The H concentration at 10 nm below the surface, where the surface oxide can be neglected, is equal to 4.8×10^{21} H/cm^3 in the as-treated sample. After annealing at 350 °C the H concentration peak is reduced to half its former value, i.e. to 2.6×10^{21} H/cm^3, while after annealing at 500 °C the H concentration peak is further reduced to 1×10^{21} H/cm^3. We note that the thermal annealing induces a partial H diffusion towards the surface; indeed the dose of incorporated H atoms decreases from 3.1×10^{15} H/cm^2 in the H_2 as-treated samples to 1.7×10^{15} H/cm^2 after the annealing at 350 °C and to 3.1×10^{14} H/cm^2 after annealing at 500 °C.

Figure 5 shows the effect of forming gas annealing on the light emission properties. The broad PL signal is initially enhanced by a factor 1.5 with annealing at lower temperatures (350°C), but then it is almost completely quenched for annealing at 500 °C.

#201767 - $15.00 USD Received 22 Nov 2013; revised 10 Feb 2014; accepted 21 Feb 2014; published 7 Apr 2014

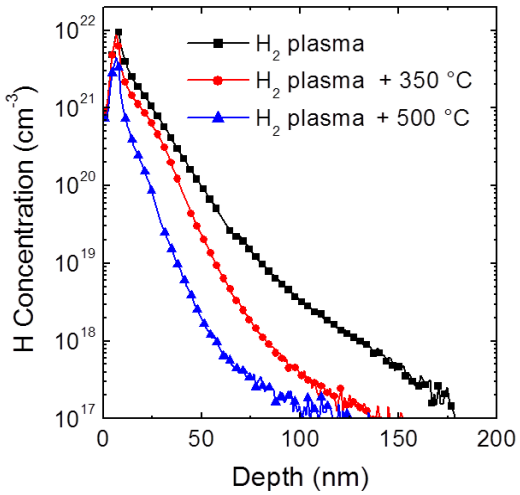

Fig. 4. H chemical profiles, as obtained by SIMS, of the H-plasma treated sample (black squares and line), after annealing at 350 °C for 30 min (red circles and line) and at 500 °C for 30 min (blue triangles and lines) in forming gas ambient.

The results obtained from the TEM, SIMS and PL analyses suggest that annealing in forming gas enhances H mobility with a double effect: from one side it promotes H evaporation from the surface but, at the same time, it increases the probability of decorating defects. At 350 °C the balance between the number of H atoms evaporated from the surface and the numbers of defects saturated by H is still positive with a consequent PL enhancement and a stabilization of platelets by the residual H in the Si layer. High temperature annealing not only results in the removal of defects, but also in the evaporation of hydrogen, since these two effects are strictly interconnected.

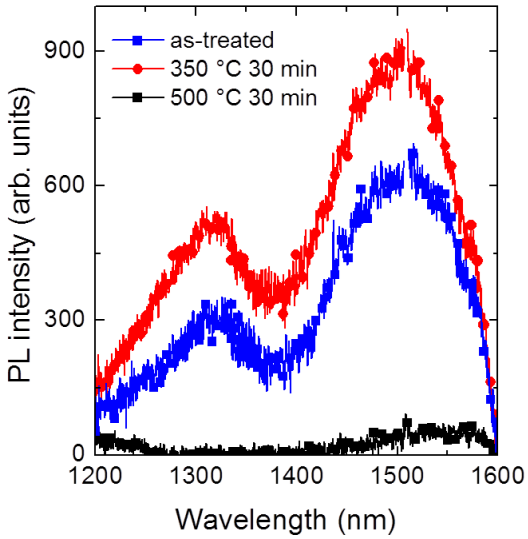

Fig. 5. Photoluminescence spectra of as-treated H-plasma SOI (blue squares and line) and after annealing at 350 °C (red circles and line) and 500 °C (black squares and line) in forming gas ambient.

#201767 - $15.00 USD Received 22 Nov 2013; revised 10 Feb 2014; accepted 21 Feb 2014; published 7 Apr 2014

3.2 H implanted SOI

We used ion implantation as a second approach to form structural defects and to incorporate hydrogen into SOI. We performed both single and multiple energy implantations. For the single implantation the energy was fixed at 8 keV in order to locate the implanted species in the center of the SOI device layer and the H fluence was varied from $1x10^{14}$ to $5x10^{15}$ H/cm^2. In order to further increase the number of emitting centres, we also performed multiple H implantations (in the energy range 5-15 keV and with doses in the range $2.3x10^{15}$ – $3.5x10^{15}$/cm^2) to widen the damaged region. These implants produce an almost constant H concentration of ~4.3 × 10^{20} H/cm^3 throughout the Si layer, comparable to the peak concentration of the single H implant with a dose of $5x10^{15}$ H/cm^2. All samples were treated in forming gas at different temperatures, ranging from 300 °C to 500 °C for 30 min, in order to find out the best annealing conditions required to maximize the PL emission.

The TEM image of a SOI sample implanted with $1x10^{14}$ H/cm^2 and annealed at 300 °C [Fig. 6(a)] does not show any extended defects. When increasing the dose up to $5x10^{15}$ H/cm^2, however, a 65 nm wide defect band, located at 85 nm below the surface, becomes apparent, as shown in Fig. 6(b). We observe extended defects consisting of (001) and {111} platelets with a mean diameter of 12 and 17 nm, respectively. The situation for the same implantation dose but for the higher annealing temperature of 500° C changes similarly as for the plasma samples [Fig. 6(c)]; the defect band is reduced to less than 40 nm extent and we observe a complete dissolution of the {111} platelets, while the mean diameter of the (001) platelets reduces to ~12 nm. For the multiple implanted samples reported in Fig. 6(d), the defect band increases, as expected, to more than 100 nm. The defect population then mainly consists of {111} platelets with a mean diameter of ~20 nm.

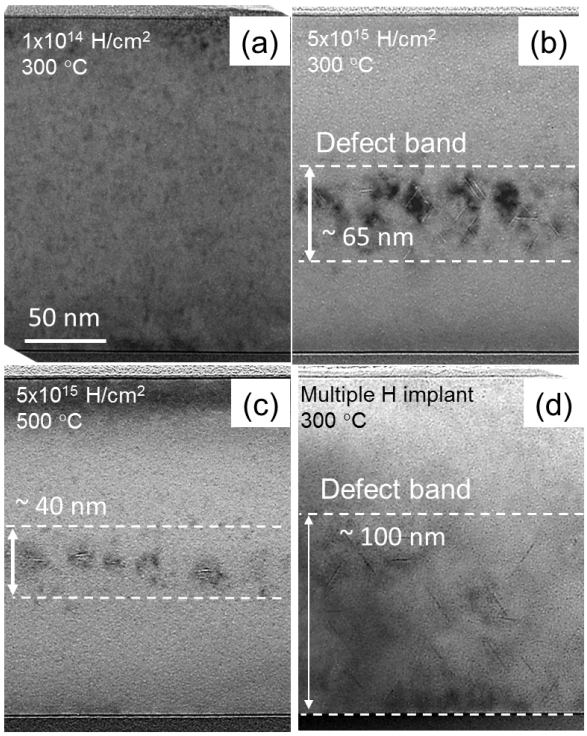

Fig. 6. Cross sectional TEM images of SOI implanted with 8 keV H to a dose of $1x10^{14}$ H/cm^2 and annealed at 300 °C (a), to a dose of $5x10^{15}$ H/cm^2 and annealed at 300 °C (b) and 500 °C (c). The CS TEM image of a SOI sample after multiple H implants and annealed at 300 °C is reported in (d).

#201767 - $15.00 USD Received 22 Nov 2013; revised 10 Feb 2014; accepted 21 Feb 2014; published 7 Apr 2014

The SIMS profiles of SOI samples implanted with $5x10^{15}$ H/cm^2 and annealed at 300 °C (red line and squares) and at 500 °C (blue line and circles) for 30 min are shown in Fig. 7. In agreement with the TEM observation, the H peak is at 110 nm below the surface with a concentration of $5x10^{20}$ H/cm^3 for the 300 °C annealed sample, while the peak concentration reduces to $2.9x10^{20}$ H/cm^3 after the annealing at 500 °C. The H integral dose following the 300 °C annealing is reduced to $2.8x10^{15}$ H/cm^2 due to H out-diffusion from the surface. Moreover, the H dose retained in correspondence of the defect band (between 85 and 150 nm below the surface) is equal to $2.2x10^{15}$ H/cm^2 and corresponds to ~85% of the total H dose, while the remaining 15% is retained in the region of Si unrelated to extended defect detected by TEM. After annealing at 500 °C, the H integral dose reduces further to $2.6x10^{14}$ H/cm^2 and the H dose trapped into defects is $1x10^{14}$ H/cm^2, corresponding to ~40 at.% of the total H dose incorporated into the Si layer. We note that these results follow the same trend as those of the plasma - treated samples shown in Fig. 4.

By comparing TEM and SIMS results obtained from both H-plasma treated and H-implanted samples, we can observe that H accumulates in correspondence to the damage. Moreover, during the thermal treatment, the thickness of the region enriched with platelets shrinks, while the H incorporated into the Si matrix progressively redistributes in the material and evaporates from the free surface. This evidence allows us to confirm that both platelets and bubbles are stabilised by H, forming Si-H bonds with the dangling bonds of Si atoms in the internal walls of each cavity and H_2 gas bubbles inside the cavity itself [21, 30].

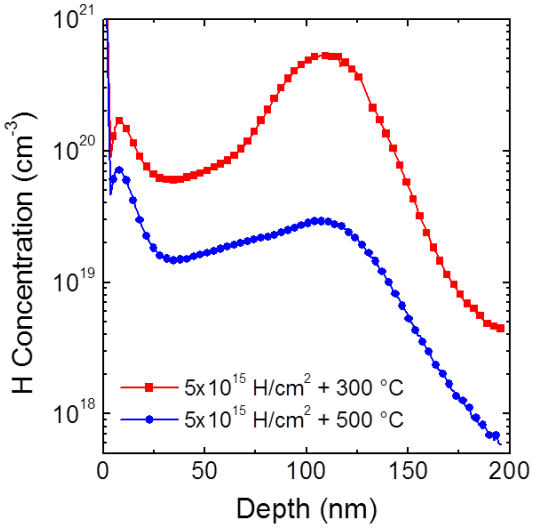

Fig. 7. H chemical profiles, as obtained by SIMS, of a SOI implanted with $5x10^{15}$ H/cm^2 and annealed at 350 °C (red squares and line) and at 500 °C (blue circles and line).

All the as-implanted SOI samples do not exhibit PL, demonstrating that the thermal treatment is essential for activating the defects formed by ion implantation. The PL spectra of H implanted samples after 300 °C annealing are shown in Fig. 8. We note the absence of any PL in the sample implanted at the lowest dose ($1x10^{14}$ H/cm^2, light blue line), while the sample implanted with $5x10^{15}$ H/cm^2 presents an intense peak at 1300 nm and a shoulder at 1500 nm (black line). Finally, we note an enhancement of PL intensity by 50% for the multiple H implanted sample, corresponding to the increase of H implanted dose. In the same figure we also show the PL spectrum of the SOI sample implanted at $5x10^{15}$ H/cm^2 after annealing at higher temperatures (500 °C, blue line), where we observe a complete suppression of the emission. In summary, the PL analyses together with the corresponding TEM micrographs give a clear evidence of the strong correlation between the PL intensity and the number of H induced defects; indeed we achieved the highest PL emission from the

#201767 - $15.00 USD Received 22 Nov 2013; revised 10 Feb 2014; accepted 21 Feb 2014; published 7 Apr 2014

multiple H implanted sample where the number of defects was maximized, as shown in Fig. 6(d). In detail, considering that whenever the {111} platelets are dissolved the PL signal decreases, we might argue that the PL activity is mainly correlated with the presence of this kind of defects.

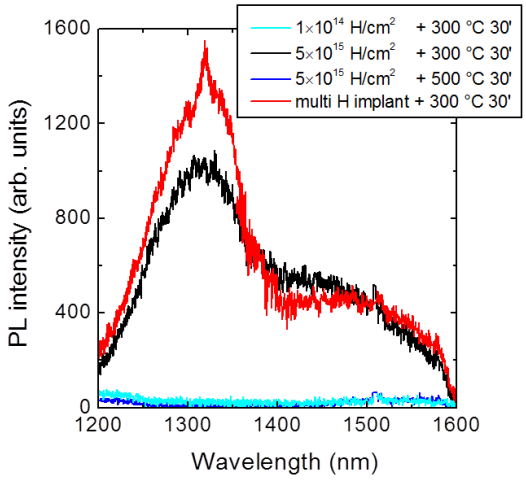

Fig. 8. Photoluminescence spectra of SOI samples implanted with a dose of $1x10^{14}$ H/cm^2 at 8 keV and annealed at 300 °C (light blue line), a dose of $5x10^{15}$ H/cm^2 and annealed at 300 °C (black line) and 500 °C (blue line). The PL spectrum of the SOI sample after multiple H implants and annealed at 300 °C is also reported (red line).

Conversely, a complete quenching of the PL, as shown in Fig. 8, is observed for samples annealed at 500 °C. The corresponding TEM images, shown in Figs. 6(a) and 6(c), highlight that the photoactive defects have almost been completely annealed out.

3.3 PL from PhC nanocavities

On the basis of all the results presented above, we can conclude that H-plasma treated SOI samples show the highest PL emission after a 350 °C annealing, while in H implanted SOI maximum PL is achieved after a 300 °C treatment. Moreover, in implanted SOI the PL band at 1300 nm is dominant, being about 4-times more intense with respect to the PL intensity than the corresponding band in the H-plasma treated SOI. This sub-bandgap optical emission, obtained after a proper material processing, can be further enhanced by inserting the optically active defects in the active region of a PhC nanocavity, following the same procedure described in [12].

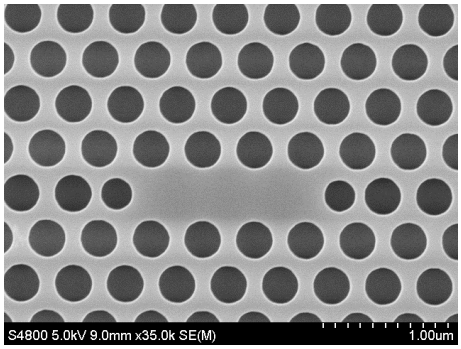

Fig. 9. SEM micrograph of a L3 PhC cavity.

For this purpose, hydrogen defects were incorporated into the L3 PhC nanocavity by both hydrogen plasma treatment and ion implantation. The cavities were designed to have their

#201767 - $15.00 USD Received 22 Nov 2013; revised 10 Feb 2014; accepted 21 Feb 2014; published 7 Apr 2014

fundamental mode in the range between 1250 and 1600 nm, in order to exploit the whole sub-bandgap optical emission band. Figure 9 shows an SEM image of one of the fabricated L3 PhC cavities.

The room temperature PL spectra of both H-plasma treated and implanted cavities are shown in Figs. 10(a) and 10(b), respectively. In both graphs, the most intense peaks are the fundamental cavity modes, as expected. The cavity modes shift towards higher wavelengths by increasing the lattice constant and their intensities approximately follow the shape of the background sub-bandgap emission. The strong PL enhancement shown by the nanocavities (about a factor 300 in the best case) is explained by the concurring effect of two mechanisms: (i) the enhancement of the extraction efficiency due to the coupling of the Si PhC slab to radiative modes, (ii) and the Purcell effect acting on the emitting centers coupled to the cavity modes [23]. Measurements performed at low temperatures (data not shown) show an overall increase of both cavity modes and background. Moreover, similarly to what reported in references [23,24,31], the background PL shows a stronger suppression with increasing temperature than the PL of cavity modes, and therefore the peak-to-background ratio monotonically increases with increasing temperature. This is a consequence of the Purcell effect, as demonstrated in ref [31]. Maximum PL intensity is observed in the PhC nanocavity fabricated in plasma-treated SOI, having a lattice constant of 400 nm (and a corresponding resonance wavelength peaked around 1450 nm). In this structure we measure a maximum power spectral density of nearly 15 pW/nm [12]. We surprisingly found that the PL of cavity modes around 1300 nm in implanted cavities is less intense than that of the plasma treated ones, contrary to what is observed in bare SOI, where the 1300 nm PL band from H-implanted SOI is more intense.

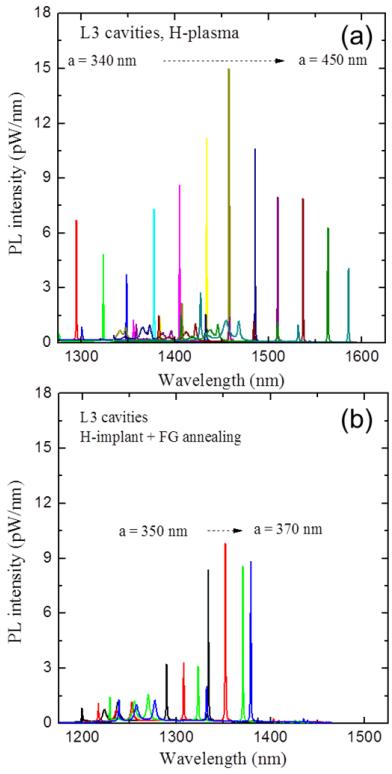

Fig. 10. Photoluminescence spectra of L3 PhC nanocavities having different lattice constant a, (a) H-plasma treated PhC cavities (b) H-implanted PhC cavities followed by thermal treatment in forming gas.

#201767 - $15.00 USD Received 22 Nov 2013; revised 10 Feb 2014; accepted 21 Feb 2014; published 7 Apr 2014

This unexpected result can be explained by considering the location of the structural defects formed inside the PhC. Cross sectional TEM performed on PhC cavities, shown in Fig. 11, allowed us to explain this unexpected result. Indeed, the weak beam dark field CS TEM (g = 400, g, 2g) of H_2 plasma treated PhC cavity reported in Fig. 11(a) shows that the isotropicity of plasma treatment induces the formation of a higher defects density close to the surface around the cavity (both on the horizontal surface and along the vertical holes sidewalls). Conversely, the bright field TEM of the implanted PhC cavity, shown in Fig. 11(b), puts in evidence that ion implantation, owing to the unidirectionality of the ion beam, creates defects only in the centre of the Si layer. Given the large surface area of the photonic crystal, the plasma treatment therefore creates more defects in the structured SOI, even though the local density may be lower, and therefore the luminescence obtained from plasma treated PhC is enhanced with respect to the implanted one.

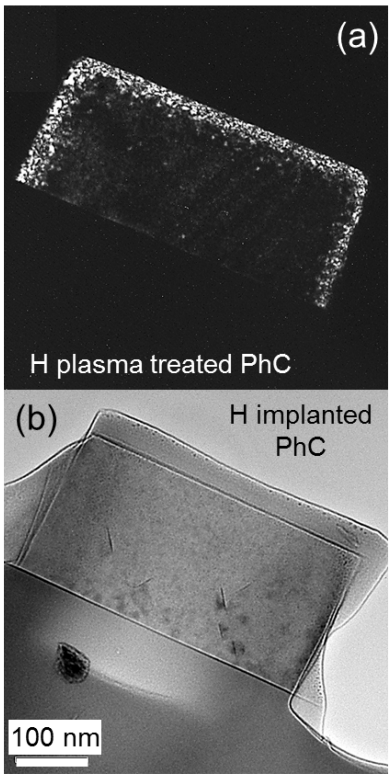

Fig. 11. Weak beam dark field cross sectional TEM (g = 400, g, 2g) of the H-plasma treated PhC cavity (a) and bright field CS TEM of the PhC cavity after multiple H implantation (b).

In addition, the Purcell enhancement depends on the spatial overlap between the distributions of the dipoles and the electromagnetic field. In particular, since the electromagnetic confinement of the fundamental cavity mode is maximum in the middle of the silicon slab, we would expect higher Purcell enhancement for emitting defects spatially located around the middle of Si slab, and therefore in H-implanted cavities (provided that the quality factor is the same). The fact that we observe the opposite result experimentally (higher PL in plasma cavities) is a clue that the higher surface-to-volume ratio and/or a larger density of defects in the plasma-treated sample is the most important mechanisms. Moreover, the fundamental role of surface-to-volume ratio is further confirmed by the comparison between the PL observed in plasma-treated samples when the treatment is made before PhC fabrication with that obtained when the plasma treatment is made after the PhC fabrication [32]. In the two cases the only difference is the surface exposed to the treatment, that is higher

#201767 - $15.00 USD Received 22 Nov 2013; revised 10 Feb 2014; accepted 21 Feb 2014; published 7 Apr 2014

when the treatment is done after the PhC fabrication. In fact a much stronger PL enhancement of the cavity mode is observed, although the broadband PL in unpatterned SOI is the same in both samples. This difference in the observed PL enhancement highlights the importance of the exposed surface area and demonstrate that the observed PL enhancement is mainly a surface effect.

4. Conclusions

In conclusion, the engineering of H induced defects formed by both plasma treatment and H implantation has been exploited in order to obtain light emission from crystalline Si. By comparing the structural and optical properties of H_2 and Ar plasma treated SOI, we clearly demonstrate that the luminescence is strictly correlated with the damage produced by the treatment. In addition, we demonstrated the advantage of using H since its passivating role reduces the non-radiative recombination. Moreover, we compared the structural and optical properties of the H_2 plasma treated and H implanted materials, demonstrating that, while ion implantation is the best method to enhance light emission in bare SOI, H_2 plasma treatment is well suited to enhance the PL from PhC cavities. Indeed, in the PhC cavity the surface/volume ratio is strongly increased with respect to a Si bulk thanks to its peculiar geometrical structure and this aspect in combination with the isotropicity of plasma allows to enhance the number of optically active defects.

These findings open the route towards the realization of monolithic silicon light sources for photonics applications.

Acknowledgments

This work was supported by Era-NET NanoSci LECSIN project coordinated by F. Priolo, by the Italian Ministry of University and Research, FIRB contract No. RBAP06L4S5 and by the EPSRC UKSp project. Partial financial support by the Norwegian Research Council is gratefully acknowledged.